Carbon consequences of forest disturbance and recovery across the conterminous United States

Christopher A. Williams,[1] G. James Collatz,[2] Jeffrey Masek,[2] and Samuel N. Goward[3]

[1] Forests of North America are thought to constitute a significant long-term sink for atmospheric carbon. The United States Forest Service Forest Inventory and Analysis (FIA) program has developed a large database of stock changes derived from consecutive estimates of growing stock volume in the U.S. These data reveal a large and relatively stable increase in forest carbon stocks over the last two decades or more. The mechanisms underlying this national increase in forest stocks may include recovery of forests from past disturbances, net increases in forest area, and growth enhancement driven by climate or fertilization by CO_2 and Nitrogen. Here we estimate the forest recovery component of the observed stock changes using FIA data on the age structure of U.S. forests and carbon stocks as a function of age. The latter are used to parameterize forest disturbance and recovery processes in a carbon cycle model. We then apply resulting disturbance/recovery dynamics to landscapes and regions based on the forest age distributions. The analysis centers on 28 representative climate settings spread about forested regions of the conterminous U.S. We estimate carbon fluxes for each region and propagate uncertainties in calibration data through to the predicted fluxes. The largest recovery-driven carbon sinks are found in the South Central, Pacific Northwest, and Pacific Southwest regions, with spatially averaged net ecosystem productivity (NEP) of about 100 g C m^{-2} a^{-1} driven by forest age structure. Carbon sinks from recovery in the Northeast and Northern Lakes States remain moderate to large owing to the legacy of historical clearing and relatively low modern disturbance rates from harvest and fire. At the continental scale, we find a conterminous U.S. forest NEP of only 0.16 Pg C a^{-1} from age structure in 2005, or only 0.047 Pg C a^{-1} of forest stock change after accounting for fire emissions and harvest transfers. Recent estimates of NEP derived from inventory stock change, harvest, and fire data show twice the NEP sink we derive from forest age distributions. We discuss possible reasons for the discrepancies including modeling errors and the possibility of climate and/or fertilization (CO_2 or N) growth enhancements.

1. Introduction

[2] The global imbalance among ocean, industrial, and land use sources/sinks of CO_2 and the amount accumulating in the atmosphere implies significant net CO_2 uptake by the terrestrial biosphere [e.g., *Schimel et al.*, 2001; *Tans et al.*, 1990]. Despite large uncertainty about magnitude and process, analyses tend to point to northern temperate and boreal lands as dominant terrestrial sinks of CO_2 but with considerable controversy regarding attribution to specific regions or continents [e.g., *Bousquet et al.*, 2000; *Fan et al.*, 1998; *Gurney et al.*, 2002; *Kaminski and Heimann*, 2001; *Myneni et al.*, 2001; *Tans et al.*, 1990]. However, some recent work suggests far smaller sinks in northern temperate and boreal lands [*Ito et al.*, 2008; *Stephens et al.*, 2007; *Yang et al.*, 2007].

[3] Estimates of the conterminous U.S. forest net carbon uptake from the atmosphere range from only 10 to over 200 Tg C a^{-1} [*U.S. Environmental Protection Agency* (*EPA*), 2010; *Houghton et al.*, 1999; *King et al.*, 2007; *Pacala et al.*, 2001; *Turner et al.*, 1995] in the last 2 decades. Note that here we consider the forest stock change alone rather than the forest sector stock change, where the latter also includes carbon accumulated in wood products (see State of the Carbon Cycle Report [*King et al.*, 2007]).

[4] Techniques for estimating forest carbon fluxes at regional to national scales include three approaches. The stock change method is exemplified in the U.S. report to the United Nations Framework Convention for Climate Change [e.g., *U.S. Environmental Protection Agency* (*EPA*), 2008]

[1]Graduate School of Geography, Clark University, Worcester, Massachusetts, USA.
[2]Biospheric Sciences Laboratory, NASA Goddard Space Flight Center, Greenbelt, Maryland, USA.
[3]Department of Geography, University of Maryland, College Park, Maryland, USA.
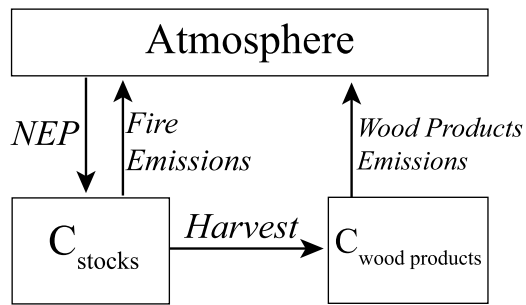
Figure 1. Schematic diagram illustrating stock and flux (italicized) relationships between the forest sector and atmosphere. The entire forest sector net flux (sink) as defined by the stock-change approach is: Net Flux = $\Delta C_{stocks} + \Delta C_{wood\ products}$. Alternatively, using our model driven estimates of *NEP* it is: Net Flux = *NEP* − *Wood Products Emissions* − *Fire*.

which uses U.S. Forest Service Forest Inventory and Analysis (FIA) data on sequential measurement of tree diameters and/or wood volumes for about 100,000 forest plots at 5–20 year intervals. Allometric and biomass expansion factors are used to convert volume into forest carbon stocks. The rate of carbon uptake is then estimated as the difference between sequential measurements divided by the number of years in the interval.

[5] Another technique for estimating forest carbon sinks combines estimates of the stand age structure of forests with age-specific carbon accumulation rates, termed the "age-accumulation" approach in this work. These carbon accumulation rates are inferred from carbon stocks as a function of age [e.g., *Houghton*, 1999], known as yield tables in forestry literature, and may be derived empirically from inventory estimates of stand volume and age or from a process oriented dynamic growth model. Finally, forest carbon sinks have been estimated from process models that account for the effects of climate variability and CO_2 and nitrogen fertilization but not necessarily for land use and disturbance processes [e.g., *Schimel et al.*, 2000]. These effects are fully contained in the stock change method because it relies on contemporary changes in stocks, but the age-accumulation approach relies on a historical characterization of carbon stock accumulation and thus misses some of the contemporary influences (see Part 4 of Text S1 in the auxiliary material).[1]

[6] Forest stock changes result from the sum of net ecosystem productivity (*NEP*), fire losses, and harvest (see Figure 1). Significant decreases in harvest and fire have not been observed over the past few decades so speculation as to the mechanisms underlying the stock increases have focused more on growth enhancement from either climate change or fertilization with elevated carbon dioxide or nitrogen [*Houghton*, 1999; *McGuire et al.*, 2001; *Nemani et al.*, 2002; *Pan et al.*, 2009; *Schimel et al.*, 2000; *Zhou et al.*, 2003] and on forest growth from post-disturbance recovery or fire suppression [*Caspersen et al.*, 2000; *Hurtt et al.*, 2002; *Pacala et al.*, 2001]. Though the growth enhancement hypothesis has been challenged by *Caspersen et al.* [2000] using forest

inventory data, others have argued that plausible rates of growth enhancement cannot be detected using existing inventories [*Joos et al.*, 2002] and recent work presents observational evidence supporting a large climate change or fertilization induced sink [*Cole et al.*, 2010; *McMahon et al.*, 2010; *Thomas et al.*, 2009].

[7] Disturbed forests, if not converted to another land cover type, have the potential to regrow, recover, or even surpass pre-disturbance carbon stocks over decades to several hundred years. The long-standing dogma of the carbon source/sink dynamics for stand-replacing disturbance involves a rapid pulse emission followed by sizable net uptake that gradually declines [*Körner*, 2003; *Odum*, 1969]. This pattern is broadly supported by chronosequence observations of carbon stocks [*Bond-Lamberty et al.*, 2004; *Gough et al.*, 2007; *Pregitzer and Euskirchen*, 2004; *Richter et al.*, 1999; *Thornton et al.*, 2002] and forest-atmosphere net CO_2 exchange [*Amiro et al.*, 2010; *Barford et al.*, 2001; *Goulden et al.*, 2011; *Law et al.*, 2003; *Schwalm et al.*, 2007], but the precise post-disturbance carbon dynamics vary by forest type and climate and this detail remains poorly characterized.

[8] The analysis reported here attempts comprehensive assessment of the carbon consequences of past and present forest disturbance and recovery across the conterminous United States. We ask if the forest age structure of the conterminous U.S. forests accounts for the stock changes reported by the FIA. Our approach utilizes the national forest inventory data (and uncertainties) to constrain the forest disturbance and recovery processes represented in an ecosystem carbon cycle model to obtain regional and national estimates of carbon consequences. The basic method can be described as having two main steps. First, we derive forest type and climate specific post-disturbance *NEP* trajectories by fitting a first-order terrestrial carbon cycle model (CASA, [*Potter et al.*, 1993; *Randerson et al.*, 1996]) to grow wood stocks consistent with FIA data. Second, these characteristic trajectories are applied to landscapes with forest age maps obtained from FIA age distributions to derive maps of *NEP* and biomass. As such, our approach corresponds to the age-accumulation method for estimating forest carbon sinks as described above. Results represent carbon dynamics of forested ecoregions across the conterminous U.S. to provide a continental-scale view of forest recovery from past disturbances. In addition, we formally propagate the uncertainty in FIA age-biomass trends using a Monte Carlo approach, as well as examine to what degree results are sensitive to uncertainty in the model's parameterization of carbon turnover time, and dependence on light, moisture, and temperature. Discrepancies between FIA estimates of stock changes and those from our age-accumulation modeling are assessed in terms of modeling errors and potential growth enhancements above and beyond recovery, similar to *Houghton* [2003].

2. Methods

2.1. Overview

[9] The core of our approach is to estimate the frequency (*F*) of land area in a region (A_{reg}), as well as the flux or stock of carbon (*Q*) each within strata of stand age, forest type (e.g., Aspen-Birch), and site productivity (high or low) (denoted with *a, f, p* subscripts). Regions are defined according to the
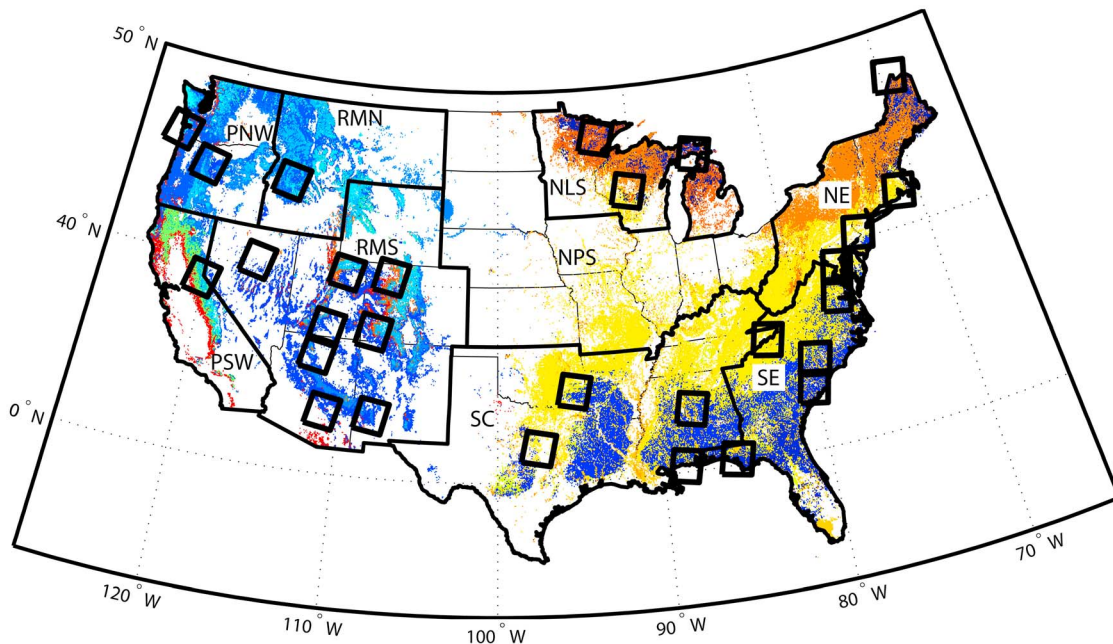
Figure 2. Conterminous U.S. distribution of forest type groups shown with thick state boundaries that trace regions from the Resource Planning Act Assessment by the U.S. Forest Service. Colors differentiate FIA forest type groups. The rectangles represent areas where gridded climate and phenology were used in the simulation of fluxes and stocks for each forest type within each rectangle.

Resource Planning Act Assessment by the U.S. Forest Service. From this we calculate the regional mass flux or stock ($Q_{reg,s}$) for a particular climate setting (subscript s) within each region, as well as its uncertainty (δ, described further below), according to

$$Q_{reg,s} = \sum_a \sum_f \sum_p Q_{afp} F_{afp} A_{reg}, \tag{1}$$

where F is the frequency of forest area adjusted to sum to unity over the three strata and obtained from the regional FIA samples of the area of forest land as described in section 2.2, A_{reg} is the total forested area in the region, and subscripts are: a for stand age, f for forest type group, and p for productivity class. The work reported here is part of a larger project to incorporate stand age derived from Landsat time series data. In this parallel effort, specific scenes for Landsat time series were obtained from a statistically rigorous sampling procedure of forest type spatially dispersed within Eastern and Western regions [Goward et al., 2008]. Here we use the climate (temperature, precipitation, incident solar radiation) and phenology for each scene (Figure 2) to simulate fluxes and stocks for each forest type and productivity class within the scene. The scenes within a region are generally good representations of the region except for the Pacific Southwest where coastal forests are not well represented. The scene level fluxes are then aggregated to regional forest fluxes and stocks by averaging across the number of climate settings (scenes, N_s) in a region as

$$Q_{reg,s} = \frac{1}{N_s} \sum_s Q_{reg,s}$$
$$\delta Q_{reg,s} = \frac{1}{N_s} \sum_s \delta Q_{reg,s}, \tag{2}$$

and conterminous U.S. estimates (subscript *nat*) are obtained from the sum over regions

$$Q_{nat} = \sum_{reg} Q_{reg}$$
$$\delta Q_{nat} = \sum_{reg} \delta Q. \tag{3}$$

We note that our estimates do not account for possible changes in forest carbon due to changes in forest area, though in section 4 we explain why this is unlikely to contribute a large carbon source or sink given the rates of current-day net land conversion.

[10] The relationship between fluxes and stocks can be diagramed as shown in Figure 1. The so-called forest sector sources/sinks refer to the net flux between the atmosphere and forest stocks plus wood products stocks. The inventory approach to calculating the net forest-atmosphere flux involves a measured change in carbon stocks over a specified period. A change in forest carbon stocks can occur because of changes in the physiological fluxes of photosynthesis and ecosystem respiration (balanced as *NEP*), as well as changes in disturbance for example by fire or harvest. *NEP* can then be inferred as the difference between ΔC_{stocks} and removals from fire and harvest. The net forest sector flux to the atmosphere is the sum of ΔC_{stocks} and $\Delta C_{wood\ products}$. This approach, used in national reports to United Nations Framework Convention on Climate Change, derives $\Delta C_{wood\ products}$ from independent harvest records and empirical decay constants for wood products and landfills.

[11] Our approach is to calibrate our modeled biomass as a function of age using forest inventory data. We then apply the biomass and associated *NEP* from forest disturbance and

recovery to the landscape based on the forest area reported by the FIA within strata of age, forest types and productivity classes within each region. In our modeling framework an important driver of ΔC_{stocks} is net primary production (NPP), and the turnover times of wood and detrital pools. NPP allocated to leaves and fine roots is quickly decomposed and cannot represent a persistent (>decadal) sink. The turnover rates of wood and its immediate detrital pool, coarse woody debris, are much slower, on the order of decades, and thus able to account for long-term net carbon fluxes (on the order of a century). Fluxes from large stocks of slowly overturning soil pools are also slow to respond to disturbance. By the time these large soil pools are affected by disturbance, recovery may have already occurred. This phenomenon is expressed as a low sensitivity of NEP to the slow turnover pools in recovering forests (see Text S1, Part 1). Of course the slow soil pools are a significant source or sink in conditions where changes in fluxes into the slow pools are large and longer term such as in permanent conversion from or to forest. This approach allows us to map NEP from recovery, one of the key atmospheric flux components needed to understand source/sink processes. NEP is a purely biological flux dependent on photosynthesis and respiration alone. Fluxes out of the forest arising from harvest or fire combine with NEP to produce net biome productivity (NBP) which is equivalent to ΔC_{stocks}. Note that we have neglected the generally smaller fluxes that contribute to NBP such as lateral fluxes of carbonate and organic matter in liquid form as well as volatile organic carbon emissions [see *Chapin et al.*, 2006].

2.2. Data Sources and Modeling

[12] Flux trajectories are derived by fitting forest growth, mortality and shedding, and allocation parameters within the Carnegie-Ames-Stanford Approach (CASA) carbon-cycle process model [*Potter et al.*, 1993; *Randerson et al.*, 1996] to accumulate carbon in aboveground wood biomass consistent with forest inventory data. Productivity in CASA is represented with a light use efficiency approach in which NPP is proportional to the fractional absorption of photosynthetically active radiation (f_{PAR}) times an efficiency term modulated by environmental conditions. NPP is allocated to leaves, roots, and wood which have specific turnover rates that reflect the delivery of carbon to nine detrital pools on the surface and in the soil. These pools decompose at specific turnover rates that are also modulated by environmental conditions. Disturbance causes NPP to initially decrease, and removes or transfers carbon between live and detrital pools, the atmosphere, and forest harvest. In this implementation, we adjust the default rate of productivity to match carbon accumulation observed in age-accumulation trajectories from forest inventory data.

[13] Inventory data were obtained from the FIA field plots (FIA Database Version 4), providing means and sampling errors for two attributes: 1) all live, oven-dry aboveground wood biomass, and 2) area of forest land. The quotient of these attributes provides biomass per unit area. Each attribute was sampled within strata of forest type group (28 classes), age (20 year age classes to 200+ years), and lumped into high and low productivity classes, defined as 120 to >225 cubic feet acre^{-1} annum^{-1} and 20 to <120 cubic feet acre^{-1} annum^{-1} respectively. Inventory samples were drawn

for regions defined by the Resource Planning Act Assessment by the U.S. Forest Service that divides the conterminous U.S. into the Northeast (NE), Southeast (SE), Northern Lakes States (NLS), South Central (SC), Northern Prairie States (NPS), Rocky Mountain North (RMN), Rocky Mountain South (RMS), Pacific Southwest (PSW), and Pacific Northwest (PNW) region (Figure 2). FIA data on forest carbon and area that are available via World Wide Web download include variances for each. However, these variances cannot be exactly combined to estimate uncertainty because of unknown covariance between carbon stock and area [*Bechtold and Patterson*, 2005]. Statisticians from the FIA (Charles Scott and colleagues, USFS National Inventory and Monitoring Applications Center) processed the national plot data to provide our study with custom products that we employed in this analysis, namely the aboveground live wood biomass per unit area and its variance for each major forest type, age cohort, productivity class, for each region shown in Figure 2. We confirmed that the data in this custom delivery were nearly identical to those obtained from other web-based data servers maintained and made available by the FIA.

[14] For this implementation we drive the CASA model with the f_{PAR} from a smoothed version of the MODIS MOD15A2 product [*Nightingale et al.*, 2009] for each forest type group as well as climatological seasonality of monthly weather using NASA Goddard Institute of Space Sciences (GISS) air temperature anomalies [*Hansen et al.*, 1999] added to a temperature climatology [*Leemans and Cramer*, 1991], GISS solar radiation [*Zhang et al.*, 2004], and Global Precipitation Climatology Project (GPCP) precipitation [*Adler et al.*, 2003]. These meteorological driver data were sampled at the 1-degree scale while f_{PAR} was provided at 1 km resolution then averaged for each forest type within each of the 28 simulation climate domains. As such, we obtain carbon flux trajectories for each combination of simulation domains (n = 28), forest-type group (n = 3 to 10), and productivity class (n = 2). Forest type group is specified at a 0.01 degree resolution obtained from *Zhu and Evans* [1994] (http://www.fia.fs.fed.us/library/maps/). Grid cell-level fractions of forest land in high and low productivity classes for each forest type and stand age within each region are specified from county level FIA data.

[15] We modified CASA to capture disturbance impacts on the carbon cycle as follows. The post-disturbance decline and ensuing recovery of NPP and fractional allocation to wood (τ) are modeled as:

$$NPP(t) = NPP_{\max}\left(1 - ce^{-kt}\right), \qquad (4)$$

$$\tau = \min[1, (t - 1)/8 \text{ years}]/3, \qquad (5)$$

where t is years since disturbance, $NPP_{\max}$ is the climatologically averaged net primary productivity independent of a disturbance legacy, c (= 1.5) determines the magnitude of disturbance-induced reduction in NPP, k (= 0.8) determines the rate of NPP recovery, and min is the minimum operator. We introduced this dynamic recovery of NPP after disturbance based on the well documented recovery of NPP [e.g., *Amiro et al.*, 2000; *Hicke et al.*, 2003]. The dynamics of allocation were intended to capture initial investment of NPP
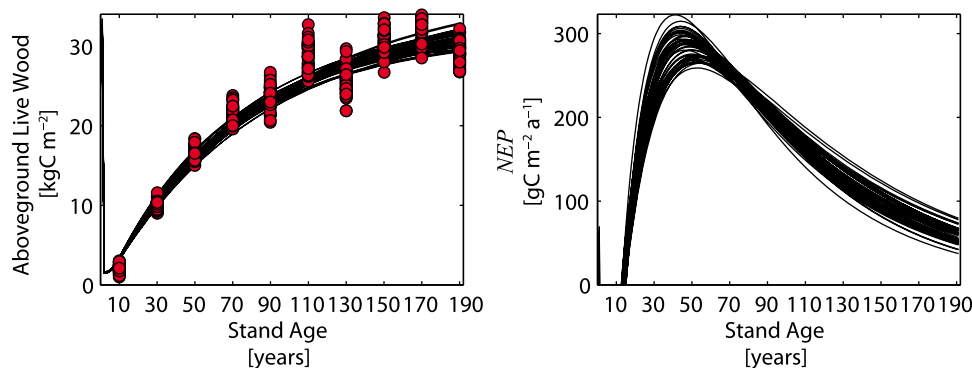
Figure 3. Characteristic trajectories of aboveground live wood biomass regrowth and associated carbon sources/sinks (expressed as net ecosystem productivity, *NEP*) following a stand-replacing disturbance in high productivity Douglas-fir stands of the Pacific Northwest. Results are from the CASA model fit to regrow stocks consistent with 25 independent samples from the forest inventory data (red circles). Net releases in the year following disturbance are as low as -3000 g C m^{-2} a^{-1} (see Text S1, Part 2, Figure A2.2) rising to above -500 g C m^{-2} a^{-1} in the second year of regrowth.

into herbaceous biomass with increasing allocation to woody vegetation with age [e.g., *Jokela et al.*, 2004; *Law et al.*, 2002].

[16] In order to parameterize the amount of biomass killed by a disturbance we adopt the following treatment. Regardless of the pre-disturbance biomass, we set the post-disturbance biomass to 50% of the aboveground live wood biomass reported in the 0–20 year age class. This constrains early regrowth to pass through the youngest age-class in the FIA sample. We then estimate the corresponding fraction of live wood, leaves, and roots killed based on the ratio of their abundance prior to disturbance relative to those immediately after disturbance. Eighty percent of the disturbance-killed aboveground wood and all of the disturbance-killed leaves are assumed to be taken off site and entrained into wood products or promptly combusted and are collectively accounted for as "removals" (fire and harvest), akin to the treatment by *Turner et al.* [1995]. The remaining 20% of disturbance-killed aboveground wood is subject to on-site post-disturbance decomposition as it enters the coarse woody debris pool, also consistent with *Turner et al.* [1995]. Disturbance-killed roots decompose on-site, for which 30% of dead coarse roots are assumed to enter a below-ground coarse woody debris pool, and 70% of dead coarse roots and all dead fine roots enter the soil metabolic and structural pools, broadly consistent with results presented by *Gough et al.* [2007] and *Meigs et al.* [2009]. We note that these and other prescriptions are uncertain, likely vary among disturbance and forest types, and are the subject of ongoing research. In summary, biomass killed in a distur-bance event is the difference between pre-disturbance bio-mass and 50% of the 0–20 year biomass reported by the FIA data. Of the killed biomass, 80% of aboveground wood and all leaves are removed (via harvest or fire) and 20% of the killed aboveground wood enters the coarse woody debris pool. The belowground wood and roots killed by disturbance remain on site to decompose. Figure 3 offers an example, in which aboveground biomass is reduced to 2.5/30 kg C m^{-2}, or <10%, and 80% of this 90% reduction in biomass is assumed to be removed (harvest or fire) while the other 20% is left to decompose on site.

[17] With this approach it is then possible to estimate biomass removals as:

$$R = A_1 B_{pre}\left(1 - f_{left}\right), \qquad (6)$$

where A_1 is the area of forested land assigned a stand age of one year based on the FIA age histogram, B_{pre} is the pre-disturbance aboveground biomass, and f_{left} ($= 0.8$) is the fraction of biomass left to decompose on-site. Each of these varies by forest type, region, and productivity class. This estimate is subject to errors in the area of forest assigned to this young age class, the age of forests prior to distur-bance and correspondingly the biomass pre-disturbance, and uncertainty in the fraction of biomass in disturbed forests that is taken off-site as wood products. Removals from non-stand replacing harvests are not considered in this approach but later in section 4 we attempt to quantify the impacts of this assumption.

[18] The next step in our model parameterization involves calculating the wood production – wood age pair that allows the best match to the inventory data of above-ground stock recovery, with the following multistep proce-dure. First, we calculate a target aboveground live wood biomass (B^*, in g C m^{-2}) from the mean in the 100 to 200 year old age classes, including successively younger age classes in 20 year increments to ensure a minimum of two samples. The target age (A^*, in years) is obtained from the average of old classes sampled to derive B^*. Second, we approximate the rate of annual aboveground live wood biomass produc-tion (P_w, in g C m^{-2} a^{-1}), which is a function of *NPP* and wood allocation, that would be required to obtain B^* by A^* for a range of possible wood turnover times (A_w) spanning 30 to 300 years in increments of 10 years by solving a simplified integral form of the differential equation for bio-mass with time (dB/d$t = P_w - B/A_w$) to yield:

$$P_w = \frac{B^*}{A_w\left(1 - e^{\frac{-A^*}{A_w}}\right)}. \qquad (7)$$

Thus, we obtain an array of possible P_w-A_w pairs that would grow the target biomass by the target age. In a few particular

cases this approach yielded implausible wood ages, but with negligible consequence for the scales of analyses presented in this study. The third step is to select the pair that provides a biomass recovery curve most like the inventory sample assessed as that which minimizes the sum of squared error between modeled and sampled aboveground live wood biomass. Modeled biomass is calculated at the sample ages (t, in years) according to:

$$B(t, A_w) = B_o e^{\frac{-t}{A_w}} + P_w A_w \left(1 - e^{\frac{-A^*}{A_w}}\right),\qquad(8)$$

where B_0 is an assumed initial biomass of 200 g C m^{-2}. Last, we linearly rescale the model's default monthly NPP values to provide an annual total NPP_{max} inferred from the fitted rate of P_w, as:

$$NPP_{max} = \frac{P_w}{\tau \alpha},\qquad(9)$$

where τ ($= 1/3$) is the allocation of NPP to wood and α ($= 0.75$) is the fraction of this that is allocated to the aboveground wood pool (stems and branches) instead of belowground (coarse roots).

[19] Following determination of P_w and A_w parameters, characteristic carbon flux trajectories (Q_{afp}) are developed from, first, a 1000 year spin-up to steady state carbon pools. This is followed by a disturbance prior to the disturbance of interest with 75 years of regrowth for all forest types except loblolly pine and longleaf/slash pine (30 years) and Douglas-fir (200 years). The age of trees at harvest is set to be just older than the typical peak in age histograms reported by the FIA (see Part 2 and Figure A2.3 in Text S1), except where harvest rotations are known to be short (SE and SC pines), or where harvest over previous decades tended to target old growth forests with high economic value (Douglas-fir [Cohen et al., 2002]). This "pre-disturbance" is important in that it establishes the amount of live carbon subject to disturbance-induced disposition, meaning taken off-site as removals or decomposing on-site. Finally, we simulate the most recent disturbance after which we allow 200 years of regrowth to characterize carbon dynamics with stand development. These procedures result in a group of carbon stock age trajectories analogous to yield tables.

[20] We have not modified CASA's default treatment of heterotrophic respiration emerging from microbial decomposition of soil and litter carbon and associated transfers among carbon pools. The general equation for the rate of heterotropic respiration from a specific carbon pool is

$$Rh_{pool} = C_{pool} k_{pool} W_{resp} T_{resp} M,\qquad(10)$$

where C_{pool} is the amount of carbon in a pool, k_{pool} is the pool-specific decay rate constant, W_{resp} and T_{resp} control how respiration depends on soil moisture and temperature states, and M is the carbon assimilation efficiency of the microbes. Total heterotrophic respiration is the sum of that from each of the nine detrital pools.

2.3. Uncertainty Analysis

[21] A formal propagation of uncertainty from sampling errors (coefficient of variation, CV) for forested area (± 10 to 100%) and total aboveground live biomass (± 10 to 100%),

and volume to carbon conversion (± 7%) are all included. The uncertainty in inventory aboveground live biomass per unit area is propagated to the predicted fluxes and aboveground live biomass with a Monte Carlo procedure analogous to Tier 2 uncertainty estimation in the IPCC Good Practice Guide [*Intergovernmental Panel on Climate Change* (*IPCC*), 2000]. The model was fit to 25 different biomass regrowth trajectories, where each trajectory was generated from random samples of the normally distributed aboveground live wood biomass for each age class (25 draws of biomass per unit area from each of 10, 20-year age classes). Forcing the fitted trajectory to conform to the assumption that biomass increases monotonically and saturates with age strongly constrains the resultant age-accumulation curves and their variances (Figure 3). An additional 7% uncertainty is used to account for tree volume to carbon conversion [*Smith and Heath*, 2001]. Put together this method involved over 130,000 simulations of age-dependent dynamics of forest carbon fluxes and stocks. The uncertainty of forest area and aboveground live biomass per unit area is obtained from the FIA data.

[22] As shown in equations (1)–(3) above, independent uncertainties in the product of flux or stock with area are combined as $\delta Q_{total} = (\frac{\delta Q_{afp}^2}{Q_{afp}^2} + \frac{\delta A_{afp}^2}{A_{afp}^2})^{1/2}$ [*Taylor*, 1997]. We adopt a conservative assumption of non-random error propagation for which uncertainty is additive over forest types, productivity classes, and ages, and also additive spatially for a simulation domain, a region, or the nation. This uncertainty aggregation is analogous to a Tier 1 uncertainty described in the IPCC Good Practice Guide [*IPCC*, 2000].

[23] Uncertainty in NEP also derives from model structure (not analyzed) as well as model parameterization of light, moisture, and temperature sensitivity of heterotrophic respiration and/or NPP expressed in the CASA model. As described in Text S1, Part 1, Section 1, we analyzed NEP responses to a 2% increase of six representative parameters including the maximum light use efficiency, moisture dependence of NPP, optimal temperature for NPP, turnover time of the slow soil carbon pool, and both the Q10 and moisture dependence of heterotrophic decomposition of soil carbon. We use a 2% change in parameter value in order to obtain a detectable response in NEP but for ease of discussion the sensitivities are divided by two and expressed as % change in NEP for a 1% change in parameter value (see Text S1, Part 1).

3. Results

3.1. Carbon Trajectories

[24] Using CASA as a controlled growth model accurately reproduces the accumulation of aboveground forest carbon stocks with time since a stand replacing disturbance as informed by FIA data (Figure 3), imposing a powerful, albeit partial, observational constraint on net ecosystem carbon flux trajectories with stand age. Additional data on litter, woody debris and soil carbon dynamics would provide much needed additional constraints on estimated ecosystem C dynamics. More rapid regrowth of aboveground stocks in the high productivity class causes higher amplitude trajectories for carbon stocks and fluxes (Figures A2.1 and A2.2 and Part 2 in Text S1) with larger post-disturbance sources

Table 1. Regional Distribution of Forest Area, Live Biomass (Live *B*), Ratio of *EPA* [2008] to This Study's Forest Area, Ratio of *EPA* [2008] to This Study's Live Biomass, Net Ecosystem Productivity (*NEP*), and Fraction of Forest That Is Less Than 25 Years Old and Less Than 5 Years Old

Region[a]	Area (10^9 m^2)	Live *B* (Tg C)	f_{EPA08} Area[b]	f_{EPA08} Live B[c]	*NEP* (Tg C a^{-1})	Percent < 25 Years	Percent < 5 Years
NE	339	3,253	1.11	1.01	32 ± 5.5	10	2
NLS	212	1,236	0.99	1.11	12 ± 1.3	16	3
SE	355	2,621	1.00	0.94	30 ± 3.5	39	8
SC	384	3,220	1.27	1.00	40 ± 4.2	37	8
RMN	192	1,189	0.98	1.10	7 ± 1.8	21	5
RMS	493	1,815	0.81	0.97	11 ± 5.5	1	0
PSW	127	1,522	1.06	0.95	13 ± 2.8	11	2
PNW	202	2,162	1.05	1.13	18 ± 3.0	19	4
Total/Mean	2,303	17,017	1.03	1.08	164 ± 27.7	17	4

[a]NE, Northeast; NLS, Northern Lakes States; SE, Southeast; SC, South Central; RMN, Rocky Mountain North; RMS, Rocky Mountain South; PSW, Pacific Southwest; PNW, Pacific Northwest.
[b]Ratio of *EPA* [2008] to this study's forest area.
[c]Ratio of *EPA* [2008] to this study's live biomass.

that give way to stronger sinks with ensuing forest regrowth. The Monte Carlo simulation approach provides an envelope of trajectories (Figure 3) that enables formal uncertainty propagation through all scales of the analysis (regional forest types to conterminous U.S. forestlands). Absolute uncertainty surrounding *NEP* tends to peak where forest uptake is maximum (peak *NEP*) and then diminishes with forest age (Figure 3). An important exception, not shown in Figure 3, is the often large uncertainty in carbon emission in the years immediately following disturbance; large because of variation in the pre-disturbance carbon stocks and the amount of dead wood that decomposes on-site. The timing of *NEP* crossover from source to sink is surprisingly insensitive to variability in biomass accumulation (not shown), and generally occurs at ages <20 years (e.g., Figure 3; Figures A2.1 and A2.2 and Part 2 in Text S1) consistent with many reported chronosequence fluxes [e.g., *Bond-Lamberty et al.*, 2004; *Gough et al.*, 2007; *Goulden et al.*, 2011; *Law et al.*, 2004; *Litvak et al.*, 2003; *Noormets et al.*, 2007; *Pregitzer and Euskirchen*, 2004]. Patterns of post-disturbance uptake of carbon in regrowing forests vary widely across regions of the conterminous U.S. as well as by forest type group and productivity class (Figures A2.1 and A2.2 and Part 2 in Text S1). Forest inventory data describing the recovery of aboveground live wood biomass carbon with stand development act as a strong constraint on the modeled carbon cycle including the rates of litter and soil carbon turnover and decay.

[25] Our analysis of the sensitivity of the model to parameters revealed that nearly all of the sensitivities are less than 1% indicating general dampening of parameter perturbations and suggesting that uncertainties in these parameterizations do not expand as they propagate through to modeled *NEP* (see Text S1, Part 1, Table A1.1). Model structure and parameter uncertainties are not included in our analysis but are expected to add about ±10% based partly on a sensitivity analysis presented in Text S1.

3.2. Continental Patterns

[26] Regional variations in disturbance rates and *NEP* across the conterminous U.S. reflect harvesting practices and regional climates (Table 1; also Table A2.1 and Figures A2.1–A2.3 in Text S1). Forests growing in relatively dry settings (e.g., Rocky Mountain South (RMS)) have low

NEP, contrasted by high carbon sequestration rates in the Pacific Southwest and Northwest, as well as Southeastern and South Central regions (Table A2.1 in Text S1). The largest rates of disturbance, and the largest sinks of carbon stimulated by forest recovery from recent disturbance ("regrowth sinks"), are in Southeastern (SE), South Central (SC), and Pacific Northwest (PNW) regions. These regional biologically driven sinks do not reflect net biome productivity because recovery trajectories do not include the fate of disturbance-induced carbon removals such as carbon taken offsite to lumber, pulp and paper mills or released promptly on-site by natural and anthropogenic fires (see schematic in Figure 1). This is addressed further in the discussion where we present the forest-to-atmosphere carbon exchange.

[27] At the continental scale, the biological recovery sink (*NEP*) is estimated to be 164 ± 28 Tg C a^{-1} (Table 1), or about 71 g C m^{-2} a^{-1} averaged for the 230 million hectares of forestland represented here. Nearly all (84%) of this *NEP* sink results from net growth of live carbon stocks with only a small fraction shared among soil carbon (6%), litter carbon (2%), and coarse woody debris (8%) stocks (Table 2). Our sample includes 93% of the conterminous U.S. forestland, reported to be 250 million hectares [*EPA*, 2008]. Our analysis did not include the Northern Prairie States region (~6% of total area and ~5% of total carbon) because the effort was originally connected to a Landsat remote sensing analysis whose random sample did not draw Landsat scenes for this region. As verification, our stand-age histograms by region generally correspond well with a similar presentation of the same basic data as recently published by *Pan et al.* [2011]. Comparing to regional statistics of forest area and live biomass reported by the *EPA* [2008] we find good correspondence overall (Table 1).

[28] The estimated uncertainty arising from forest area, aboveground wood biomass, and conversion of diameter measurements to volume and carbon produced relatively small uncertainty estimates in our biomass and fluxes. This is partly due to the continuous, monotonically increasing, and saturating growth form imposed by the process-model approach. This functional form is more plausible than one that would allow abrupt increases and decreases in aboveground live wood biomass with stand development (i.e., stand age) as are commonly found in the inventory data when arrayed as a chronosequence (e.g., Figure 3, 110–150 year

Table 2. Changes in Carbon Stocks (Tg C a^{-1}) in the Year 2005 Reported in Different Studies

	This Study	EPA [2008]
ΔTotal Soil C	3	9
ΔLitter C	1	15
ΔCoarse Woody Debris (CWD)	4	16
ΔCWD Below	0	−
ΔLive C	39	133
Total Stock Change	47	173
Removals[a]	117	162
Harvest[b]	107[c]	132
Wildfire Emissions[d]	10	30
NEP[e]	164	335
Wood Products Emissions[f]	102	102
Wood Products Storage[g]	5	30
Forest Sector-Atmosphere Exchange[h]	52	203

[a]For EPA [2008] calculated as: Removals = Wildfire Emissions + Harvest.

[b]This study inferred as: Harvest = Removals − Wildfire Emissions.

[c]Italicized values are inferred from mass balance.

[d]This study estimated wildfire emissions from the Global Fire Emissions Database v3 (GFED3) [van der Werf et al., 2010].

[e]For the purposes of this table calculated as NEP = ΔTotal Soil C + ΔLitter C + ΔCWD + ΔCWD Below + ΔLive C + Removals; values differ from those in Table 1 due to differences in the method of aggregation and associated averaging of terms.

[f]This study adopted values reported by the EPA [2008].

[g]This study calculated as Wood Products Storage = Removals − Wood Products Emissions − Wildfire Emissions.

[h]This study calculated as Forest Sector-Atmosphere Exchange = NEP − Wood Products Emissions − Wildfire Emissions.

biomass). Imposing the model's growth form has the effect of filtering out some of the variance inherent in chronosequence trajectories of biomass with stand age. Other uncertainties arising from model structure and assumptions about disturbance severity/type, age, partial cutting, natural wood turnover, and a possible age-related decline in productivity are evaluated by judging the impacts of these factors on model output through sensitivity analyses (see Text S1, Part 1, Section 2).

[29] We used the 1km forest type map to produce a gridded map of NEP and its uncertainty (from variances in FIA data) for the conterminous U.S. (Figure 4). Within each region each forest type considered was assigned the regional estimate of NEP for that forest type and region. Regional forest NEP sinks range from >25 to 200 g C m^{-2} a^{-1} with eastern and western forests generally ranging from 75 to 100 g C m^{-2} a^{-1}. The RMS region is predicted to be uniformly <50 g C m^{-2} a^{-1}. The discontinuities conforming to state borders between West Virginia and Virginia and between Washington and Idaho occur because the same forest types in each neighboring region have regionally specific and different growth and disturbance rates.

[30] As an independent evaluation of our predicted stocks and fluxes we compared our results with five available studies on chronosequences for forest types in the conterminous U.S.. These studies sometimes do not include estimates of both fluxes and stocks for different aged forests and estimates used various biometric and flux measurement approaches. The small number of sites with available data, variability in the data, and issues of extrapolating fine scale measurements to regional responses do not justify quantitative comparisons and demonstrate the need for more of these types of measurements and for finer scale modeling. The

results of these comparisons are shown in Text S1, Part 3, Figure A3.1. Agreement varies widely between the comparisons at the different sites/regions.

4. Discussion

[31] Comparing estimates of the conterminous U.S. forest NEP sink from multiple studies (Table 3) reveals a general separation between age-accumulation and stock-change methods. This comparison spans estimates for the 1980s to more recent years (e.g., 2005–2006), but this may be justified because atmospheric inversions seem to indicate a long-term mean sink in North America during the '80s and '90s but with large interannual variability [Baker et al., 2006]. Four of the six age dependent analyses that seek to represent carbon emissions and sequestration with post-disturbance recovery provide lower estimates of the forest NEP sink when compared to the four stock-change analyses, with 82 g C m^{-2} a^{-1} versus 154 g C m^{-2} a^{-1} averaged across their respective studies, or 189 Tg C a^{-1} versus 354 Tg C a^{-1} when integrated across U.S. forest area. This is even true when process-oriented studies rely on forest inventory data to prescribe the rate of aboveground carbon stock recovery with time, as well as the area of forest of different ages. For example, regarding NEP alone we find general agreement with Turner et al. [1995] who reported 203 Tg C a^{-1} compared to our estimate of 164 Tg C a^{-1}. In contrast, the EPA [2008] stock-change estimate of forest NEP is twice as large as this study's age-accumulation result (335 compared to 164 Tg C a^{-1}, Table 2). The disparity between the stock-change method and these other, age-accumulation results is likely due to large annual to decadal increases in stocks measured in the inventory that then implies greater NEP (regrowth). What causes this general disagreement remains unclear, though growth enhancement is a plausible explanation of the difference, consistent with recent publications [Cole et al., 2010; Luyssaert et al., 2010; McMahon et al., 2010; Thomas et al., 2009]. Effects of growth enhancement are implicit in the stock-change method but not well incorporated in the age-accumulation methods that emphasize effects of regrowth dynamics, even when these methods rely on inventory-derived chronosequences to constrain biomass accumulation as in the present study (see Part 4 in Text S1 for an illustration of this). There is also one study reported in Table 3 including only the effects of climate and CO_2 fertilization based on an ensemble of models for the conterminous U.S. [Schimel et al., 2000]. If this sink were added to the forest recovery (age-yield table) estimates the results would be more in line with the stock change approach.

[32] We note that the EPA [2008] estimate of total removals is 38% higher than that estimated with our modeling approach (= 162/117, Table 3). About half of the difference is due to elevated fire emissions reported by the EPA [2008], however this estimate is much higher than the rate of forest fire emissions being reported elsewhere [e.g., van der Werf et al., 2010]. This difference translates directly into the NEP estimated from the stock change method, and elevates the EPA [2008] estimate by 20 TgC a^{-1} relative to the estimate from our approach. The EPA [2008] report also estimates 25 TgC a^{-1} greater removals by harvest. There are two ways we could adjust our methodology to try to match this rate of removal. We could either, a) increase the amount
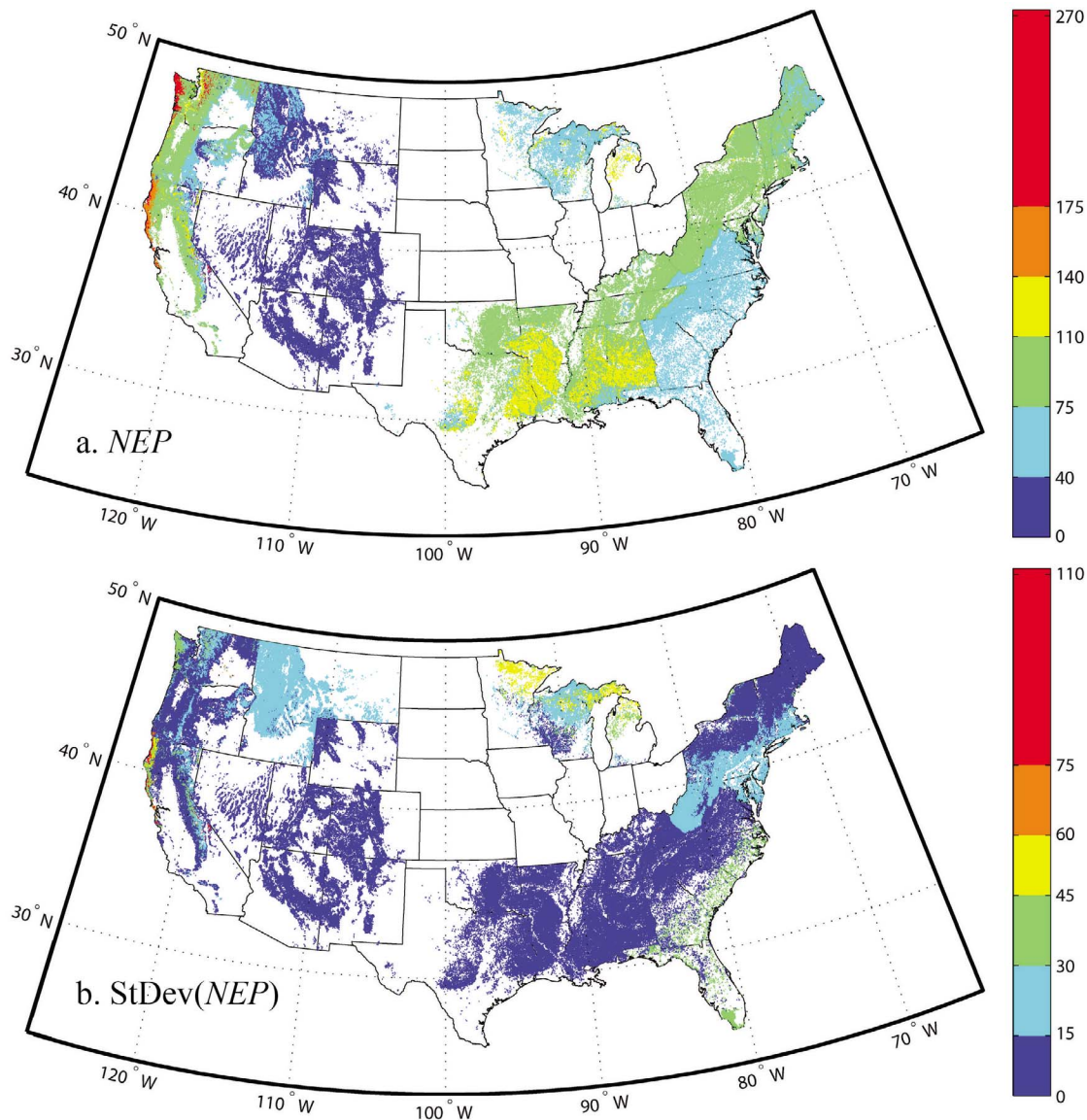
Figure 4. Map of average (a) net ecosystem productivity and (b) uncertainty expressed as one standard deviation (*NEP* in g C m^{-2} a^{-1}) for forests of the conterminous U.S.

of biomass removed by disturbances on average by increasing the age and hence biomass of disturbed forests, b) increase the amount of biomass removed on average by removing a larger fraction of pre-disturbance biomass and leaving less to decompose on site, or c) increase the area of forests disturbed by increasing the young-aged fraction of forests if we believe the stand age attribute offers a biased representation. All of these would increase removals but they would have different effects on *NEP*. The first option would decrease *NEP* because more disturbance-killed material would be left on-site to decompose and be emitted from forests. The second approach would increase *NEP* because of reduced on-site decomposition. The third approach would decrease *NEP* because a larger fraction of forested area would be concentrated at young stand ages (<15 year old) where *NEP* is either a large negative value or near zero (Figures A2.1 and A2.2 in Text S1). And in the extreme case that we simply adjusted our *NEP* estimate upwards to cover

the difference in removals, the *EPA* [2008] estimate would still be 126 TgC a^{-1} higher than the estimate emerging from our age-accumulation method.

[33] A term-by-term comparison between stock changes reported from inventory methods and those derived in the current study's age-accumulation approach indicates that a change in live carbon stocks makes up a large portion of the difference in *NEP* estimated with the two methods (Table 2). Annual increases in soil carbon, coarse woody debris, and litter pools are also noticeably lower in the present analysis compared to those reported by the *EPA* [2008; 2010] (Table 3). Because our method, necessarily, produces aboveground live wood biomass and forest area estimates that are consistent with, or wholly derived from, the inventory itself (Table 1), our relatively low estimate of annual changes in live stocks (Table 2) does not appear to be caused by underestimation of a) stocks, or b) forest area. These differences translate to the full forest sector-

Table 3. Forest Carbon *NEP* and Stock Change for the Conterminous U.S. (Tg C a^{-1}) From This and a Sample of Previously Published Estimates[a]

Source	Approach	Mean *NEP*	Low	High	ΔC_{stocks}	Harvest	Fire
Schimel et al. [2000][b]	*P*	80					
This Study[c]	*AA*	164	136	192	47	107	10
Houghton et al. [1999][d]	*AA*	182			10	92	80
Turner et al. [1995][e]	*AA*	203			79	124	0
Houghton [2003][f]	*AA*	207			35	92	80
Woodbury et al. [2007][g]	ΔC_{stocks}	270	256	293	108	132	30
EPA [2008][g]	ΔC_{stocks}	335			173	132	30
Birdsey and Heath [1995][h]	ΔC_{stocks}	368			211	127	30
Hurtt et al. [2002][d]	*AA*	372	282	442	230	92	50
Pacala et al. [2001][d]	synthesis	392	312	472	220	92	80
King et al. [2007][d]	ΔC_{stocks}	411	383	439	236	145	30

[a]Estimates are classified according to approach: age structure–C accumulation (*AA*), stock change (ΔC_{stocks} = NBP), or process model (*P*), where *P* is a process model ensemble result that accounts for CO_2 and climate effects [*Schimel et al.*, 2000; *Pacala et al.*, 2001] and combines approaches for an overall estimate and range. Low and High refers to 1 standard deviation about the mean estimate.
[b]For 1980–1993.
[c]For 2005, C stock change = *NEP* − *Harvest* − *Fire* (see Table 2), our total removals are 117 Tg C a^{-1} that includes fire and harvest, assume fire at 10 Tg C a^{-1} (see GFED3 of *van der Werf et al.* [2010] and *Zheng et al.* [2011]).
[d]For the 1980s.
[e]For ~1990.
[f]For 1990s, harvest and fire from *Houghton et al.* [1999].
[g]For 2005.
[h]For 1992.

atmosphere net exchange, whereby the stock-change method estimates a much larger forest sector C sink than obtained with this study's age-accumulation approach (Table 2).

[34] Our maps of conterminous U.S. forest *NEP* and its uncertainty (Figure 4) are one of the first of which we are aware (though see *Woodbury et al.* [2007]) and will be used in further study of the impact of the forest disturbance fluxes on atmospheric CO_2 as a boundary flux for atmospheric transport models much as gridded fire, fossil fuel burning, and ocean CO_2 fluxes are prescribed in forward and inverse atmospheric modeling [e.g., *Peters et al.*, 2007]. Complete accounting of forest sector fluxes would additionally require maps of fire [e.g., *van der Werf et al.*, 2010] and wood products emissions. These studies will allow assessment of the detection limits for the magnitude and spatial variability of sinks in top-down studies.

[35] This study's approach imposed a number of simplifying assumptions that were necessary given the initial scope of our work. Below we address some of these and their potential implications regarding interpretation of our results.

[36] (1) We assume characteristic regrowth trajectories regardless of disturbance type even though the nature of post-disturbance carbon dynamics is sure to vary between fire, harvest, hurricane, and the severity of disturbance. For instance, around twice as much coarse woody debris (CWD) may remain on site after a severe fire compared to clear-cut harvest [*Tinker and Knight*, 2000]. This remaining detritus provides a source of CO_2 for a prolonged period after disturbance. Using data reported by *Smith et al.* [2009] and the National Interagency Fire Center (to account for Alaskan fires) we estimate that for the year 2004 the ratio of burned area to harvested area in the eastern U.S. was about 0.30 compared to 0.46 in the west. In terms of carbon removals though, our forest fire estimates from the Global Fire Emissions Database v3 (10 Tg C a^{-1}) are much smaller than our estimated harvest removals (107 Tg C a^{-1}). Because the total removals are dominated by harvest, as is the total area disturbed, accounting for differences caused by fire versus

harvest would not significantly change our results or conclusions. Furthermore, some but not all of this variation is captured by the Monte Carlo approach, as well as with stratification by site productivity and across regions. Partial disturbances such as defoliation events are not represented with the current methodology, and discussed further below.

[37] (2) Our assumption of equivalence between forest age and time since disturbance does not account for the effects of partial disturbance that allows older aged trees to remain among regenerating cohorts or the dynamic state of old forests that have reached the age of natural mortality and reestablishment. This particular issue has been examined by *Bradford et al.* [2008] for a subalpine forest system. In that study a large part of the age versus years since disturbance discrepancy arose in stands undisturbed for long periods of time (>200 years), longer than what we analyze in this work. From FIA data we estimate that about 3% of forested land is >200 years old for conterminous U.S.

[38] (3) Our analysis is sensitive to biases in the ages associated with the aboveground live wood biomass trajectories, as explored in an extensive sensitivity analysis described in Text S1, Part 1, Section 2. For instance, if the FIA ages are older (younger) than actual stand ages, our predicted recovery sink is underestimated (overestimated). This, of course, is an issue with any approach proposing to use FIA age structure information to estimate fluxes and stocks [e.g., *Pan et al.*, 2011]. Despite this sensitivity, we note that bias in stand age is not likely to be large enough to explain the major differences between the stock-change and age-accumulation methods (Table A1.2 in Text S1).

[39] (4) The FIA data we used to construct aboveground live wood biomass trajectories include the effects of partial cuts, which are a significant component of disturbance in U.S. forests contributing >50% of the total harvested area [*Smith et al.*, 2009]. Reported stand ages reflect the trees not cut while the plot level biomass will be lower in these cases producing lower regional aboveground live wood biomass for mid and older aged stands. These partial cutting practices

(e.g., salvage logging, selective logging, thinning), which remove biomass from forested plots without resetting the FIA-recorded stand age, could have a substantial influence on the forest *NEP* estimate. The implicit inclusion of plots that experienced partial cutting (not fully stocked) likely results in correct biomass estimates but lowers the slope of regrowth trajectories resulting in some underestimation of *NEP*. In an extensive sensitivity analysis (Text S1, Part 1, Section 2) we find strong sensitivity to such biases, with a 10% elevation of biomass leading to a 14% elevation of conterminous U.S. forest *NEP*. This is equivalent to a 2.3 Tg C a^{-1} increase in *NEP* for each 1% increase in biomass. Despite this large sensitivity to biomass trajectories, to account for the approximately 160 Tg C a^{-1} difference, the reported biomass would need to have been underestimated by 70% (= 160 Tg C a^{-1}/2.3 Tg C a^{-1} per 1% increase in biomass). Additional sensitivity analyses examining effects of natural, partial disturbances that lead to wood turnover and on site decomposition (e.g., ice storms, blowdowns, insect damage) indicate that they are also unlikely to present a large error/bias in our estimate.

[40] (5) We do not take into account annual changes in forest area which could contribute to the discrepancy between recovery and stock change approaches. The *EPA* [2008] reports indicate that forest area has been increasing at a rate of 0.24% a^{-1} since 1990. If we assume that new forests would range between 1 to 5 kg C m^{-2} over an age range of 0 to 20 years (e.g., see Figure 3) then the average accumulation rate for these forest would be about 250 g C m^{-2} a^{-1}. Correcting this for the increase in forest area produces an added 1.7 Tg C a^{-1} sink, indistinguishable within the uncertainties of our method.

[41] (6) It has been proposed that forest carbon sinks may be driven by long-term trends in temperature, precipitation, nitrogen deposition, and atmospheric CO_2. Responses to these trends are embedded in the biomass-age trajectories from the inventories in complex ways and more recent increases in growth may not be accounted for in our approach (see Text S1, Part 4 for a thorough examination of this). Others have addressed this and concluded that forests are not responding in a systematic way to these trends [*Caspersen et al.*, 2000], that forest inventory data are not precise enough to resolve expected responses to trends [*Joos et al.*, 2002], and that a smaller number of inventory measurements on forests of known disturbance history do indeed show strong trends in growth enhancement correlated with trends in temperature and atmospheric CO_2 [*McMahon et al.*, 2010; *Thomas et al.*, 2009]. In a study of global terrestrial carbon sinks using CASA, *Thompson et al.* [1996] showed that in order to obtain a terrestrial carbon sink of ∼2 Pg C/yr broadly consistent with top-down sink estimates, *NPP* has to undergo a sustained increase of 0.18% per annum. Similar estimates have been reported by others [e.g., *Joos et al.*, 2002]. Our own sensitivity analysis (not shown) showed that a sustained increase in *NPP* of 0.2% per annum would increase live biomass in a typical 60 year old forest by approximately 5% and is thus a weak or undetectable signal in a biomass chronosequence. A 0.2% annual increase in *NPP* is implausibly large sensitivity of photosynthesis to CO_2 (*dNPP/NPP* x CO_2/*d*CO_2 of ∼0.96, or near proportional response) and would require other positive feedback

mechanisms such as nitrogen fertilization and/or climate trends to operate in parallel. We conclude that plausible responses of forest sinks to climate and CO_2 or N cannot be resolved with FIA biomass-age trajectories alone such as those we utilize here and that have been proposed by others [e.g., *Pan et al.*, 2011].

[42] The approach described here is also sensitive to uncertain parameters including rates of wood mortality and coarse woody debris decomposition, as well as the amount of dead aboveground and belowground biomass left to decompose onsite following disturbance. It lacks a standing dead wood pool that may be important because it decomposes much more slowly than dead wood in contact with the forest floor [e.g., *Harmon and Hua*, 1991; *Harmon et al.*, 2004; *Janisch et al.*, 2005]. In our ongoing efforts, literature is being exhaustively explored to better constrain these and other parameters and processes. Additional effort is being invested in attributing disturbances to particular drivers based on spatial and geospatial records of fire and insect outbreaks. While valuable, it is unlikely that such refinements and constraints will reconcile the large differences between the age-accumulation and stock-change approaches, something that may benefit from a close collaboration with inventory experts to clarify differences of approach and accounting, as well as more comprehensive assessment of possible growth enhancement effects. Future efforts at improving this study's approach will include more detailed prescriptions of type and severity of disturbances, further comparisons with site observations as they become available, and analyses of top-down atmospheric constraints on source/sink magnitude and distributions. Estimates would also be better constrained if additional data on litter, dead wood and soil organic carbon dynamics were available from field studies.

5. Conclusions

[43] Forest Inventory and Analysis data provide unique and valuable information about disturbance history and associated carbon stocks and fluxes with forest recovery. By using these data to constrain forest growth rates in a carbon cycle model, this study provides a more detailed estimate of carbon sources and sinks from recent forest disturbance and recovery across regions and forest types of the U.S.. One of our key findings is a much smaller net sink of carbon in conterminous U.S. forests than previously estimated with the stock-change approach as used in UNFCCC reporting [*EPA*, 2008]. The source of across study inconsistencies among national estimates of stocks and fluxes remains largely unexplained. The paucity of observed net ecosystem productivity and biomass chronosequences limits our ability to evaluate modeled responses. These types of observations are critically needed in order to adequately test models representing disturbance and subsequent recovery.

References

Adler, R., et al. (2003), The Version-2 Global Precipitation Climatology Project (GPCP) monthly precipitation analysis (1979–present), *J. Hydrometeorol.*, 4(6), 1147–1167, doi:10.1175/1525-7541(2003)004<1147: TVGPCP>2.0.CO;2.

Amiro, B. D., et al. (2000), Net primary productivity following forest fire for Canadian ecoregions, *Can. J. For. Res.*, 30(6), 939–947, doi:10.1139/x00-025.

Amiro, B. D., et al. (2010), Ecosystem carbon dioxide fluxes after disturbance in forests of North America, *J. Geophys. Res.*, 115, G00K02, doi:10.1029/2010JG001390.

Baker, D. F., et al. (2006), TransCom 3 inversion intercomparison: Impact of transport model errors on the interannual variability of regional CO2 fluxes, 1988–2003, *Global Biogeochem. Cycles*, 20, GB1002, doi:10.1029/2004GB002439.

Barford, C., et al. (2001), Factors controlling long- and short-term sequestration of atmospheric CO2 in a mid-latitude forest, *Science*, 294, 1688–1691, doi:10.1126/science.1062962.

Bechtold, W. A., and P. L. Patterson (2005), The enhanced Forest Inventory and Analysis Program—National sampling design and estimation procedures, *SRS GTR-80*, U.S. Dep. of Agric. For. Serv., South. Res. Stn., Asheville, N. C.

Birdsey, R. A., and L. S. Heath (1995), Carbon changes in U.S. forests, in *Productivity of America's Forests and Climate Change*, Tech. Rep. RM-271, edited by L. A. Joyce, pp. 56–70, U.S. Dep. of Agric. For. Serv., Rocky Mt. For. and Range Exp. Stn. Fort Collins, Colo.

Bond-Lamberty, B., et al. (2004), Net primary production and net ecosystem production of a boreal black spruce wildfire chronosequence, *Global Change Biol.*, 10, 473–487, doi:10.1111/j.1529-8817.2003.0742.x.

Bousquet, P., et al. (2000), Regional changes in carbon dioxide fluxes of land and oceans since 1980, *Science*, 290(5495), 1342–1346, doi:10.1126/science.290.5495.1342.

Bradford, J. B., et al. (2008), Tree age, disturbance history, and carbon stocks and fluxes in subalpine Rocky Mountain forests, *Global Change Biol.*, 14, 2882–2897, doi:10.1111/j.1365-2486.2008.01686.x.

Caspersen, J. P., et al. (2000), Contributions of land-use history to carbon accumulation in U.S. forests, *Science*, 290(5494), 1148–1151, doi:10.1126/science.290.5494.1148.

Chapin, F. S., III, et al. (2006), Reconciling carbon-cycle concepts, terminology, and methods, *Ecosystems*, 9, 1041–1050, doi:10.1007/s10021-005-0105-7.

Cohen, W., et al. (2002), Characterizing 23 years (1972–95) of stand replacement disturbance in western Oregon forests with Landsat imagery, *Ecosystems*, 5, 122–137, doi:10.1007/s10021-001-0060-X.

Cole, C. T., et al. (2010), Rising concentrations of atmospheric CO$_2$ have increased growth in natural stands of quaking aspen (*Populus tremuloides*), *Global Change Biol.*, 16, 2186–2197, doi:10.1111/j.1365-2486.2009.02103.x.

Fan, S., et al. (1998), A large terrestrial carbon sink in North America implied by atmospheric and oceanic carbon dioxide data and models, *Science*, 282, 442–446, doi:10.1126/science.282.5388.442.

Gough, C. M., et al. (2007), The legacy of harvest and fire on ecosystem carbon storage in a northern temperate forest, *Global Change Biol.*, 13, 1935–1949, doi:10.1111/j.1365-2486.2007.01406.x.

Goulden, M. L., et al. (2011), Patterns of NPP, GPP, respiration, and NEP during boreal forest succession, *Global Change Biol.*, 17, 855–871, doi:10.1111/j.1365-2486.2010.02274.x.

Goward, S. N., et al. (2008), Forest disturbance and North American carbon flux, *Eos Trans. AGU*, 89(11), 105, doi:10.1029/2008EO110001.

Gurney, K. R., et al. (2002), Towards robust regional estimates of CO2 sources and sinks using atmospheric transport models, *Nature*, 415(6872), 626–630, doi:10.1038/415626a.

Hansen, J., R. Ruedy, J. Glascoe, and M. Sato (1999), GISS analysis of surface temperature change, *J. Geophys. Res.*, 104, 30,997–31,022, doi:10.1029/1999JD900835.

Harmon, M. E., and C. Hua (1991), Coarse woody debris dynamics in two old-growth ecosystems, *BioScience*, 41(9), 604–610, doi:10.2307/1311697.

Harmon, M. E., et al. (2004), Production, respiration, and overall carbon balance in an old-growth Pseudotsuga-Tsuga forest ecosystem, *Ecosystems*, 7, 498–512.

Hicke, J. A., et al. (2003), Postfire response of North American boreal forest net primary productivity analyzed with satellite observations, *Global Change Biol.*, 9(8), 1145–1157, doi:10.1046/j.1365-2486.2003.00658.x.

Houghton, R. A. (1999), The annual net flux of carbon to the atmosphere from changes in land use 1850–1990, *Tellus, Ser. B*, 51(2), 298–313, doi:10.1034/j.1600-0889.1999.00013.x.

Houghton, R. A. (2003), Why are estimates of the terrestrial carbon balance so different?, *Global Change Biol.*, 9(4), 500–509, doi:10.1046/j.1365-2486.2003.00620.x.

Houghton, R. A., et al. (1999), The U.S. carbon budget: Contributions from land-use change, *Science*, 285(5427), 574–578, doi:10.1126/science.285.5427.574.

Hurtt, G. C., et al. (2002), Projecting the future of the U.S. carbon sink, *Proc. Natl. Acad. Sci. U. S. A.*, 99(3), 1389–1394, doi:10.1073/pnas.012249999.

Intergovernmental Panel on Climate Change (IPCC) (2000), Good practice guidance and uncertainty management in national greenhouse gas inventories, edited by J. Penman et al., Inst. for Global Environ. Strategies, Kanagawa, Japan.

Ito, A., et al. (2008), Can we reconcile differences in estimates of carbon fluxes from land-use change and forestry for the 1990s?, *Atmos. Chem. Phys.*, 8, 3291–3310, doi:10.5194/acp-8-3291-2008.

Janisch, J. E., et al. (2005), Decomposition of coarse woody debris originating by clearcutting of an old-growth conifer forest, *Ecoscience*, 12(2), 151–160, doi:10.2980/i1195-6860-12-2-151.1.

Jokela, E. J., et al. (2004), Production dynamics of intensively managed loblolly pine stands in the southern United States: A synthesis of seven long-term experiments, *For. Ecol. Manage.*, 192, 117–130, doi:10.1016/j.foreco.2004.01.007.

Joos, F., et al. (2002), Growth enhancement due to global atmospheric change as predicted by terrestrial ecosystem models: Consistent with US forest inventory data, *Global Change Biol.*, 8, 299–303, doi:10.1046/j.1354-1013.2002.00505.x.

Kaminski, T., and M. Heimann (2001), Inverse modeling of atmospheric carbon dioxide fluxes, *Science*, 294, 259, doi:10.1126/science.294.5541.259a.

King, A. W., et al. (Eds.) (2007), The first state of the carbon cycle report (SOCCR): The North American carbon budget and implications for the global carbon cycle, synthesis and assessment product 2.2, http://cdiac.ornl.gov/SOCCR/, Natl. Oceanic Atmos. Adm., Natl. Clim. Data Cent., Asheville, N. C.

Körner, C. (2003), Slow in, rapid out—Carbon flux studies and Kyoto targets, *Science*, 300, 1242–1243, doi:10.1126/science.1084460.

Law, B. E., et al. (2002), Environmental controls over carbon dioxide and water vapor exchange of terrestrial vegetation, *Agric. For. Meteorol.*, 113(1–4), 97–120, doi:10.1016/S0168-1923(02)00104-1.

Law, B. E., et al. (2003), Changes in carbon storage and fluxes in a chronosequence of ponderosa pine, *Global Change Biol.*, 9, 510–524, doi:10.1046/j.1365-2486.2003.00624.x.

Law, B. E., et al. (2004), Disturbance and climate effects on carbon stocks and fluxes across Western Oregon USA, *Global Change Biol.*, 10, 1429–1444, doi:10.1111/j.1365-2486.2004.00822.x.

Leemans, R., and W. P. Cramer (1991), The IIASA database for mean monthly values of temperature, precipitation and cloudiness of a global terrestrial grid, *Rep. RR-91-18*, 62 pp., Int. Inst. for Appl. Syst. Anal., Laxenburg, Austria.

Litvak, M., S. Miller, S. C. Wofsy, and M. Goulden (2003), Effect of stand age on whole ecosystem CO$_2$ exchange in the Canadian boreal forest, *J. Geophys. Res.*, 108(D3), 8225, doi:10.1029/2001JD000854.

Luyssaert, S., et al. (2010), The European carbon balance. Part 3: Forests, *Global Change Biol.*, 16, 1429–1450, doi:10.1111/j.1365-2486.2009.02056.x.

McGuire, A. D., et al. (2001), Carbon balance of the terrestrial biosphere in the Twentieth Century: Analyses of CO$_2$, climate and land use effects with four process-based ecosystem models, *Global Biogeochem. Cycles*, 15(1), 183–206, doi:10.1029/2000GB001298.

McMahon, S. M., et al. (2010), Evidence for a recent increase in forest growth, *Proc. Natl. Acad. Sci. U. S. A.*, 107(8), 3611–3615, doi:10.1073/pnas.0912376107.

Meigs, G. W., et al. (2009), Forest fire impacts on carbon uptake, storage, and emission: The role of burn severity in the Eastern Cascades, Oregon, *Ecosystems*, 12, 1246–1267, doi:10.1007/s10021-009-9285-x.

Myneni, R. B., et al. (2001), A large carbon sink in the woody biomass of northern forests, *Proc. Natl. Acad. Sci. U. S. A.*, 98(26), 14,784–14,789, doi:10.1073/pnas.261555198.

Nemani, R., M. White, P. Thornton, K. Nishida, S. Reddy, J. Jenkins, and S. Running (2002), Recent trends in hydrologic balance have enhanced the terrestrial carbon sink in the United States, *Geophys. Res. Lett.*, 29(10), 1468, doi:10.1029/2002GL014867.

Nightingale, J. M., et al. (2009), Temporally smoothed and gap-filled MODIS land products for carbon modelling: Application of the *f*PAR product, *Int. J. Remote Sens.*, 30, 1083–1090, doi:10.1080/01431160802398064.

Noormets, A., et al. (2007), Age-related changes in forest carbon fluxes in a managed northern Wisconsin landscape, *Ecosystems*, 10, 187–203, doi:10.1007/s10021-007-9018-y.

Odum, E. (1969), The strategy of ecosystem development, *Science*, 164, 262–270, doi:10.1126/science.164.3877.262.

Pacala, S. W., et al. (2001), Consistent land- and atmosphere-based U.S. carbon sink estimates, *Science*, 292(5525), 2316–2320, doi:10.1126/science.1057320.

Pan, Y., et al. (2009), Separating effects of changes in atmospheric composition, climate and land-use on carbon sequestration of U.S. Mid-Atlantic temperate forests, *For. Ecol. Manage.*, *259*, 151–164, doi:10.1016/j.foreco.2009.09.049.

Pan, Y., et al. (2011), Age structure and disturbance legacy of North American forests, *Biogeosciences*, *8*, 715–732, doi:10.5194/bg-8-715-2011.

Peters, W., et al. (2007), An atmospheric perspective on North American carbon dioxide exchange: CarbonTracker, *Proc. Natl. Acad. Sci. U. S. A.*, *104*, 18,925–18,930, doi:10.1073/pnas.0708986104.

Potter, C. S., J. T. Randerson, C. B. Field, P. A. Matson, P. M. Vitousek, H. A. Mooney, and S. A. Klooster (1993), Terrestrial Ecosystem Production: A process model based on global satellite and surface data, *Global Biogeochem. Cycles*, *7*(4), 811–841, doi:10.1029/93GB02725.

Pregitzer, K. S., and E. S. Euskirchen (2004), Carbon cycling and storage in world forests: Biome patterns related to forest age, *Global Change Biol.*, *10*, 2052–2077, doi:10.1111/j.1365-2486.2004.00866.x.

Randerson, J. T., M. V. Thompson, C. M. Malmstrom, C. B. Field, and I. Y. Fung (1996), Substrate limitations for heterotrophs: Implications for models that estimate the seasonal cycle of atmospheric CO_2, *Global Biogeochem. Cycles*, *10*(4), 585–602, doi:10.1029/96GB01981.

Richter, D. D., et al. (1999), Rapid accumulation and turnover of soil carbon in a re-establishing forest, *Nature*, *400*, 56–58, doi:10.1038/21867.

Schimel, D., et al. (2000), Contribution of increasing CO_2 and climate to carbon storage by ecosystems in the United States, *Science*, *287*(5460), 2004–2006, doi:10.1126/science.287.5460.2004.

Schimel, D. S., et al. (2001), Recent patterns and mechanisms of carbon exchange by terrestrial ecosystems, *Nature*, *414*(6860), 169–172, doi:10.1038/35102500.

Schwalm, C. R., et al. (2007), A method for deriving net primary productivity and component respiratory fluxes from tower-based eddy covariance data: A case study using a 17-year data record from a Douglas-fir chronosequence, *Global Change Biol.*, *13*, 370–385, doi:10.1111/j.1365-2486.2006.01298.x.

Smith, J. E., and L. S. Heath (2001), Identifying influences on model uncertainty: An application using a forest carbon budget model, *Environ. Manage. N. Y.*, *27*(2), 253–267, doi:10.1007/s002670010147.

Smith, W. B., et al. (2009), Forest resources of the United States, *Gen. Tech. Rep. WO-78*, 336 pp., U.S. Dep. of Agric. For. Serv., Washington, D. C.

Stephens, B. B., et al. (2007), Weak northern and strong tropical land carbon uptake from vertical profiles of atmospheric CO_2, *Science*, *316*, 1732–1735, doi:10.1126/science.1137004.

Tans, P. P., et al. (1990), Observational constraints on the global atmospheric CO_2 budget, *Science*, *247*(4949), 1431–1438, doi:10.1126/science.247.4949.1431.

Taylor, J. R. (1997), *An Introduction to Error Analysis: The Study of Uncertainties in Physical Measurements*, 2nd ed., 326 pp., Univ. Sci. Books, Sausilito, Calif.

Thomas, R. Q., et al. (2009), Increased tree carbon storage in response to nitrogen deposition in the US, *Nat. Geosci.*, *3*, 13–17, doi:10.1038/ngeo721.

Thompson, M. V., J. T. Randerson, C. M. Malmström, and C. B. Field (1996), Change in net primary production and heterotrophic respiration: How much is necessary to sustain the terrestrial carbon sink?, *Global Biogeochem. Cycles*, *10*(4), 711–726, doi:10.1029/96GB01667.

Thornton, P. E., et al. (2002), Modeling and measuring the effects of disturbance history and climate on carbon and water budgets in evergreen needleleaf forests, *Agric. For. Meteorol.*, *113*(1–4), 185–222, doi:10.1016/S0168-1923(02)00108-9.

Tinker, D. B., and D. H. Knight (2000), Coarse woody debris following fire and logging in Wyoming lodgepole pine forests, *Ecosystems*, *3*, 472–483, doi:10.1007/s100210000041.

Turner, D. P., et al. (1995), A carbon budget for forests of the conterminous United States, *Ecol. Appl.*, *5*(2), 421–436, doi:10.2307/1942033.

U.S. Environmental Protection Agency (EPA) (2008), Inventory of U.S. greenhouse gas emissions and sinks: 1990–2006, 394 pp., Washington, D. C.

U.S. Environmental Protection Agency (EPA) (2010), Inventory of U.S. greenhouse gas emissions and sinks: 1990–2008, *EPA 430-R-10-006*, Off. of Atmos. Prog., Washington, D. C.

van der Werf, G. R., et al. (2010), Global fire emissions and the contribution of deforestation, savanna, forest, agricultural, and peat fires (1997–2009), *Atmos. Chem. Phys.*, *10*, 11,707–11,735, doi:10.5194/acp-10-11707-2010.

Woodbury, P. B., et al. (2007), Carbon sequestration in the U.S. forest sector from 1990 to 2010, *For. Ecol. Manage.*, *241*, 14–27, doi:10.1016/j.foreco.2006.12.008.

Yang, Z., R. A. Washenfelder, G. Keppel-Aleks, N. Y. Krakauer, J. T. Randerson, P. P. Tans, C. Sweeney, and P. O. Wennberg (2007), New constraints on Northern Hemisphere growing season net flux, *Geophys. Res. Lett.*, *34*, L12807, doi:10.1029/2007GL029742.

Zhang, Y.-C., W. B. Rossow, A. A. Lacis, V. Oinas, and M. I. Mishchenko (2004), Calculation of radiative fluxes from the surface to top of atmosphere based on ISCCP and other global data sets: Refinements of the radiative transfer model and the input data, *J. Geophys. Res.*, *109*, D19105, doi:10.1029/2003JD004457.

Zheng, D., et al. (2011), Carbon changes in conterminous US forests associated with growth and major disturbances: 1992–2001, *Environ. Res. Lett.*, *6*, 014012, doi:10.1088/1748-9326/6/1/014012.

Zhou, L., R. K. Kaufmann, Y. Tian, R. B. Myneni, and C. J. Tucker (2003), Relation between interannual variations in satellite measures of northern forest greenness and climate between 1982 and 1999, *J. Geophys. Res.*, *108*(D1), 4004, doi:10.1029/2002JD002510.

Zhu, Z., and D. L. Evans (1994), U.S. forest types and predicted percent forest cover from AVHRR data, *Photogramm. Eng. Remote Sens.*, *60*, 525–531.

G. J. Collatz and J. Masek, Biospheric Sciences Laboratory, NASA Goddard Space Flight Center, Code 618, Greenbelt, MD 20771, USA.

S. N. Goward, Department of Geography, University of Maryland, 2181 LeFrak Hall, College Park, MD 20782, USA.

C. A. Williams, Graduate School of Geography, Clark University, 950 Main St., Worcester, MA 01610, USA. (cwilliams@clarku.edu)